

An interpretable semi-supervised classifier using two different strategies for amended self-labeling

Isel Grau · Dipankar Sengupta ·
María M. García Lorenzo · Ann Nowé

January 26th, 2020

Abstract In the context of some machine learning applications, obtaining data instances is a relatively easy process but labeling them could become quite expensive or tedious. Such scenarios lead to datasets with few labeled instances and a larger number of unlabeled ones. Semi-supervised classification techniques combine labeled and unlabeled data during the learning phase in order to increase classifier’s generalization capability. Regrettably, most successful semi-supervised classifiers do not allow explaining their outcome, thus behaving like black boxes. However, there is an increasing number of problem domains in which experts demand a clear understanding of the decision process. In this paper, we report on an extended experimental study presenting an interpretable self-labeling grey-box classifier that uses a black box to estimate the missing class labels and a white box to make the final predictions. Two different approaches for amending the self-labeling process are explored: a first one based on the confidence of the black box and the latter one based on measures from Rough Set Theory. The results of the extended experimental study support the interpretability by means of transparency and simplicity of

This work was supported by the IMAGica project, financed by the Interdisciplinary Research Programs and Platforms (IRP) funds of the Vrije Universiteit Brussel; and the BRIGHT-analysis project, funded by the European Regional Development Fund (ERDF) and the Brussels-Capital Region as part of the 2014-2020 operational program through the F11-08 project ICITY-RDI.BRU (icity.brussels).

I. Grau
Vrije Universiteit Brussel, Belgium
E-mail: igraugar@vub.be

D. Sengupta
Vrije Universiteit Brussel, Pleinlaan 2 1050 Brussel, Belgium
Centre for Cancer Research and Cell Biology, Queens University Belfast, United Kingdom

M.M. García Lorenzo
Universidad Central “Marta Abreu” de Las Villas, Cuba

A. Nowé
Vrije Universiteit Brussel, Belgium

our classifier, while attaining superior prediction rates when compared with state-of-the-art self-labeling classifiers reported in the literature.

Keywords Semi-supervised Classification · Self-labeling · Interpretability · Explainable Artificial Intelligence · Black Box Model · Grey Box Model · Rough Sets Theory

1 Introduction

Gathering data examples for training a machine learning classifier in a real-world scenario is often simple, but the process of assigning labels to the examples can be costly in terms of money, time or effort. In such scenarios we might obtain datasets with more unlabeled than labeled data. This is often the case in applications such as image classification [27], industrial fault classification [68], sentiment analysis [66], speaker identification [19] and bioinformatics or medical applications [65]. Semi-supervised classification (SSC) techniques arise from the need to address this problem using both labeled and unlabeled data for training a classifier. The aim is to increase the generalization ability of the classifier when compared to a supervised classifier that only uses the available labeled data.

The SSC literature reports several techniques including transductive Support Vector Machines [5], Graph-based methods [6], Generative Mixture Models [24], Self-labeling techniques [57] and more recently semi-supervised Generative Adversarial Networks [55]. More details on the related work are given in Section 2. By and large, state-of-the-art SSC methods involve three main shortcomings that may vary from a specific family of algorithms to the whole field. The first issue affecting all SSC models refers to the assumption that the unlabeled data share the same distribution as the labeled instances. Secondly, some techniques such as transductive Support Vector Machines or Graph-based methods mainly focus on transductive learning, i.e. predicting the label for a given set of unlabeled data rather than finding a model capable of predicting the classification of unseen instances with a proper generalization. Thirdly, while self-labeling approaches such as Co-training [33], Self-training [67] and their variants perform quite well in terms of accuracy, they often result in complex structures combining several classifiers and failing to give the user insight in how the classification process comes about.

An increasing requirement observed in machine learning is to obtain not only precise models but also interpretable ones. End users often demand an insight into how an algorithm arrives at a particular outcome and need an explanation of the decisions to some extent. In general, explainable artificial intelligence is starting to be a central concern in both governing and research communities. For example, the EU General Data Protection Regulation includes a right to obtain an explanation on the decisions made by an algorithm affecting human beings [30]. This regulation might limit the potential of using artificial intelligence in a variety of domains, unless we start developing more transparent models.

Although recent studies [17, 26, 45] attempted to formalize terms such as interpretability or explainability, a common conclusion is that a certain grade of global interpretability can be reached through the use of more transparent techniques as proxies for solving a task. In this paper, we refer to such models (e.g., linear regression, decision trees or rule induction algorithms) as white boxes, as opposed to the less interpretable black-box ones (e.g. artificial neural networks or support vector machines). Black boxes are normally more accurate techniques that learn exclusively from data but they are not easily understandable at a global level. Whereas white boxes refer to models which are constructed based on laws or principles of the problem domain, or those who are built from data but their structure allows for explanations or interpretation, since pure white boxes rarely exists [47]. Another alternative to reach interpretability is using white boxes as surrogates [46] for distilling previously trained black boxes. While the former strategy attempts to explain the problem domain directly, the latter is devoted to explain the domain by approximating the predictions produced by a black-box classifier.

In this paper, we study the SSC problem from the interpretability angle. We conduct a detailed revision of methods reported in the literature and discuss their shortcomings when interpretability comes to play. We explore the performance of our semi-supervised classifier termed *self-labeling grey-box* (SIGb) [31, 32], which exploits the strength of black-box models being good classifiers with the interpretability of white boxes. In terms of interpretability, we refer to a grey-box model as the combination of a black-box model with a white-box one. Our classifier uses a black box to estimate the decision class for unlabeled instances in order to increase the amount of training data. Afterwards, our approach builds a surrogate white-box classifier from the enlarged dataset that allows explaining the predictions. In addition we explore the effects of using two weighting strategies to reduce the effect of misclassifications when building the enlarged dataset. The former is based on the black box’s confidence for the inferred class label, while the latter is based on granular computing principles. The use of an enlarged dataset combined with a weighting strategy results in a white box with improved prediction rates. Numerical experiments using 55 datasets in different settings show that our proposal attains a good balance between prediction rates and explainability, while outperforming most state-of-the-art methods.

The rest of this paper is structured as follows. Section 2 provides an overview of state-of-the-art SSC algorithms reported in the literature and their interpretability, while making emphasis on self-labeling techniques. Section 3 describes the SIGb approach and Section 4 depicts two alternatives for the amending of the self-labeling performed by the black-box classifier. Section 5 introduces the numerical simulations and an extensive discussion covering the performance and interpretability of the SIGb. Section 6 formalizes the concluding remarks and research directions to be explored in the future.

2 Semi-supervised classification methods and interpretability

In supervised classification the goal is to identify the right category (among those in a predefined set) to which an observation belongs. These observations (henceforth called instances) are often described by a set of numerical and/or nominal attributes. Solving this problem implies to define a mapping $f : X \rightarrow Y$ that assigns to each instance $x \in X$, described by a set of attributes $A = \{a_1 \dots, a_p\}$, a decision class $y \in Y$. The mapping is learned from data in a supervised fashion, i.e., by relying on a set of previously labeled examples, used to train the classifier.

Semi-supervised techniques attempt to use both labeled and unlabeled instances during the learning process for increasing the prediction capacity when only labeled data is used. More formally, in a SSC scenario we have a set of m instances $L = \{l_1, \dots, l_m\}$ which are associated with their respective class labels in Y , and a set of n unlabeled instances $U = \{u_1, \dots, u_n\}$, where usually $n > m$. In the context of SSC, the classifier performance can be evaluated in two settings: (1) transductive learning, which only attempts to predict the labels for the given unlabeled instances in U ; or (2) inductive learning, which tries to infer a mapping $g : L \cup U \rightarrow Y$ for predicting the class label of any instance associated with the classification problem.

In this section, we review the main state-of-the-art methods for semi-supervised classification, including an analysis of their interpretability. Here, we evaluate the interpretability as the inherent model transparency, as described in [45].

2.1 Semi-supervised classification methods

As mentioned, SSC methods often involve assumptions about the distribution or characteristics of the unlabeled data [73]. For example, transductive Support Vector Machines (tSVMs) [5] assume that the decision boundary lies in a low-density region. This method uses unlabeled data for maximizing the margin between the different classes by placing the decision boundaries in sparse regions. However, given the fact that the complexity of the optimization problem increases in the semi-supervised setting, its computational burden is quite high and it does not scale well for large-scale data. Recent studies [10, 44] try to overcome this limitation by using the concave-convex procedure and variations of stochastic gradient descent to solve the optimization problem. From the interpretability point of view, this method has the drawback of behaving as a complete black box.

Graph-based methods [6] assume that high-dimensional data lie on a low-dimensional manifold [13]. These methods represent the data space as a graph (i.e., if two instances are strongly connected, then they likely belong to the same class) and estimate a continuous function which is close enough to the label values, with the ultimate goal of propagating labels between similar instances. Recent works on Label Propagation methods [28, 18] are mainly

focused on the construction of an effective graph over data with complex distribution and reducing the risk of error propagation through outliers. This approach could be interpretable to some extent by visually inspecting the obtained graph from the structural point of view, allowing some transparency at the parameters level. However, graph-based methods are mainly devoted to the transductive setting.

A third approach assumes that the data follow an identifiable mixture distribution (Generative Mixture Models [24]), henceforth they learn a joint probability for identifying the mixture components using the unlabeled data. This approach may be convenient when the available data produce well-separated clusters [73], but most of the time the joint distribution is not easily identifiable. Here the estimated mixture distribution could be interpretable at a very high abstraction level if the representation space of the problem at hand is not too complex. However, the unlabeled data could have a negative effect on algorithm’s performance if the generative model is wrong.

More recently, deep architectures have been explored by extending graph-based methods [60] and generative models [40]. Particularly successful has been the extension of Generative Adversarial Networks (GAN) [29] to the SSC context [49, 55]. For example, Feature Matching GANs [55] use a discriminator for $c + 1$ labels instead of the binary “real/fake” distinction, where the first c are the class labels of the problem and $c + 1$ corresponds to the generated instances. Despite their relative success in the SSC field, it is still unclear whether a good generator and a good discriminator for semi-supervised learning can be obtained at the same time [16]. However, the interpretability of deep learning techniques has been confined to the context of the image features representation at different layer levels or by means of post-hoc methods [11].

Self-labeling refers to a wide family of very powerful and versatile wrapper methods that employ one or more base classifiers for enlarging the available labeled dataset assuming the predictions they produce on the unlabeled data are correct. Since our contribution falls within this category, we decided to revise those SSC methods in a separate subsection to gain in clarity.

2.2 Self-labeling techniques

According to [57], self-labeling techniques can be categorized into single-view or multi-view methods based on whether they need one or multiple datasets for learning. Self-training approaches [67] are single-view wrapper classifiers, which rely on the prediction of only one base classifier to repeatedly increase the size of the labeled dataset by predicting the unlabeled instances. The instances are added incrementally, in batch [34] or in an amending procedure [42]. The use of amending procedures allows selecting or weighting the self-labeled instances for enlarging the labeled dataset, hence avoiding error propagation.

The multi-view methods assume that the data space can be described from two or more different viewpoints. These different views normally correspond to

distinct sets of attributes describing the same instances [63]. A classic example of multi-view methods is the Co-training [7] approach, where different classifiers are trained separately, each using a different attribute subset. Thereafter, the prediction of each classifier over the unlabeled dataset is used for enlarging the training set of the other. Other alternatives using multiple classifiers but not needing multi-view datasets are Democratic Co-learning [71], Tri-training [72], Co-training by committee [33] and Co-Forest [43] which use several base classifiers of the same type. Tri-training uses three base classifiers that collaborate in the learning process by labeling an unlabeled example if the other two classifiers agree. An alternative to Co-training is Co-training by committee, which does not require multi-view nor different learning algorithms, and explores different ensemble strategies with Bagging as the best performing one. Similarly, Co-Forest adopts a Random Forest classifier as an alternative for Co-training.

Self-labeling techniques are easy to implement and apply to almost all existing classifiers [20, 1, 38, 58]. A wide experiment conducted in [57] shows that CoTraining using Support Vector Machines as a base classifier [33], TriTraining using C4.5 decision tree [72], CoBagging using C4.5 [33] and Democratic Co-learning (as an ensemble of Naïve Bayes, C4.5 and K-Nearest Neighbors) [71], are the best performing self-labeling classifiers evaluated against a comprehensive collection of benchmark datasets. Other semi-supervised classifiers that have demonstrated competitive performance in a variety of datasets are self-training using logistic model trees [20], differential evolution [64] or naive Bayes [38].

In terms of interpretability, a self-training scheme producing a simulatable model (e.g., relatively simple tree structure) as the final classifier can be considered a transparent model. More complex schema such as Tri-training, Co-Bagging, Co-Forest or Co-training are less likely to be interpretable due to the collaborative nature of the algorithms and the complexity of the resulting structure. However, the ensemble character of self-labeling is a perfect match with the use of local or global surrogate models for explaining predictions. Combining base classifiers using self-labeling in a way that the resulting ensemble works as a surrogate white box is the challenge we want to address. In the next section, we describe a simple yet effective self-labeling method which uses two base classifiers, a black box and a white box, for reaching a suitable trade-off between performance and interpretability.

3 Self-labeling grey-box approach

In this section we describe the *self-labeling grey-box* proposed in our previous works [31]¹. Here, we use a black-box classifier to predict the decision class of

¹ The authors in [52] report on an ensemble grey-box strongly inspired in our previous work [31]. They claim that their main contribution is the use of the confidence of the black box predictions as amending of the self-labeling, however this idea was earlier proposed in our previous work [32]. The only difference between their method and our model is that

the unlabeled instances, while a surrogate white box is used to build an interpretable predictive model (e.g., a rule-based approach), based on the whole instance set. The aim is to outperform the base white-box component using only the originally labeled data, while maintaining a good balance between performance and interpretability. It is worth mentioning that the main motivation behind SIGb is not to outperform the most complicated state-of-the-art algorithms but to provide a simple and elegant approach allowing for interpretability. In other words, we should be able to produce competitive solutions without significantly increasing the complexity inherent to the base classifiers.

The learning process is performed in a sequential order. In a first step, we provide the available labeled dataset (L, Y) to a black-box classifier for training. Once the supervised learning is completed, the black-box component has learned a function $f : L \rightarrow Y$, where $f \in F$, being F the hypothesis space that associates each instance with a class label. The f function can be computed from the scoring function $h : L \times Y \rightarrow [0, 1]$ such that $f(x) = \operatorname{argmax}_{y \in Y} \{h(l, y)\}, l \in L$. Thereafter, the trained black-box component is used for generating new tuples (u, y) by mapping all unlabeled instances $u \in U$ to a class label $y \in Y$ as $y = f(u)$, adding a self-labeling character to the approach. From this step we obtain an enlarged training set $(L \cup U, Y)$ comprising the original labeled instances and the extra labeled ones.

In the second step, the enlarged training set $(L \cup U, Y)$ is used to train a surrogate white-box classifier. Once the learning process in the white-box component is completed, we obtain a function $g : (L \cup U) \rightarrow Y$ resulting in a classifier which is more likely to have better generalization capabilities than the original white-box component, when trained on only the labeled data. Figure 1 summarizes this process.

When applying self-labeling, we should be aware of the risk of having imbalanced data with respect to the class labels. It might be easier to obtain unlabeled data of a certain class, for example, in the context of credit fraud detection or rare diseases classification. In order to deal with this problem, our approach additionally incorporates a simple strategy for balancing instances as a preprocessing step. This weight is computed as:

$$w_{(l_j, y_i)} = |L_{[y_{min}]}| / |L_{[y_i]}| \quad (1)$$

where $L_{[y_i]}, L_{[y_{min}]} \subset L$ denote the sets of labeled instances that are mapped to the class label y_i and the minority class y_{min} , respectively. In this way we assign higher importance to instances belonging to the minority class.

In general, the SIGb approach is only based on the general assumption of SSC methods: the distribution of unlabeled instances helps elucidate the distribution of all examples. In addition, our approach allows retaining the inherent interpretability of the chosen white-box surrogate. According to the taxonomy proposed in [57], our approach can be categorized as follows:

they use an iterative process to select the instances to be included in the enlarged dataset. However, this seems to be a strange approach considering that the confidence amending reduces the need of such an iterative process.

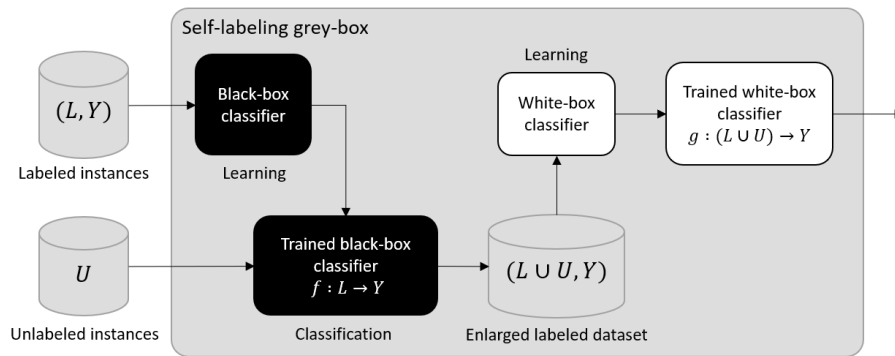


Fig. 1: General architecture of the SIGb approach. Labeled data is used for training a black-box classifier, which assigns labels to the unlabeled data. A white-box surrogate model is trained on the enlarged dataset for obtaining a interpretable model.

single-view: the SIGb classifier does not need different attribute sets for describing the instances, adding simplicity to the model;

multi-classifier: two different base classifiers are used, connected in a sequential process, the first classifier should be a good performing black-box supervised classifier, whereas the second should be a white-box technique guaranteeing interpretability to the final model;

multi-learning: the learning process comprises two steps, where two different learning algorithms are used depending on the base classifiers.

It can be noticed that the performance of the whole SIGb approach largely depends on the prediction capability of the black-box classifier when classifying unseen instances. Obviously, like any other machine learning algorithm, when solving application problems the performance will also depend on the quality of the data and the application of domain-dependent preprocessing steps [41]. However, in the context of self-labeling, the classification mistakes can reinforce themselves if no amending procedure is used during self-training. Therefore, in the next section we describe two amending strategies for the self-labeled instances, in order to prevent the error from propagating through the model.

4 Amending strategies

In this section, we describe two strategies for weighting the instances that result from the self-training stage. The goal is to improve the quality of the final model either in terms of performance or interpretability. The first strategy uses the confidence of the predictions made by the base black box and the second one focuses on the possible inconsistency of the enlarged dataset. Therefore, both procedures assign more importance to more reliable instances

in the second learning step, avoiding the propagation of errors or inconsistent information.

4.1 Using the calibrated probabilities of the black-box classifier

For the first strategy, the amending process for each unlabeled instance u is based on the probability of belonging to a certain class, which is computed by the black-box classifier in the self-labeling. The weights are assigned to the instances after they are labeled by the black-box classifier, thus expressing the confidence degree associated to the self-labeling process. Equation (2) shows how to compute the weight $w_{(u_k, y_i)}$ using the scoring function of the black-box base classifier $h(u_k, y_i)$ that expresses the calibrated probability of u_k being correctly assigned to the y_i class,

$$w_{(u_k, y_i)} = h(u_k, y_i). \quad (2)$$

As a matter of fact, this amending strategy comprises an alternative to the use of incremental or batch procedures, thus reducing the computational burden of the self-labeling process. The pseudocode in Algorithm 1 formalizes the SlGb approach incorporating this step.

```

Data: Labeled instances  $(L, Y)$ , Unlabeled instances  $U$ 
Result:  $g : (L \cup U) \rightarrow Y$ 
begin
  /* Preprocessing: Weight labeled instances according to Eq. (1) */
  forall  $(l_j, y_i) \in (L, Y)$  do
    |  $w_{(l_j, y_i)} \leftarrow |L_{min}|/|L_i|$ 
  end
  /* Train black-box component with weighted labeled data */
   $f, h \leftarrow \text{blackboxClassifier.fit}(L, Y, w)$ 
  /* Self-labeling process: Assign a label to unlabeled instances using
  black-box inference */
  forall  $u_k \in U$  do
    |  $y_i \leftarrow f(u_k)$ 
    | /* Compute weight of instance  $u_k$  according to Eq.(2) */
    |  $w_{(u_k, y_i)} \leftarrow h(u_k, y_i)$ 
    | /* Add the instance to enlarge dataset */
    |  $(L \cup U, Y) \cup \{(u_k, y_i)\}$ 
  end
  /* Train white-box component with the weighted  $(L \cup U, Y)$  dataset */
   $g \leftarrow \text{whiteboxClassifier.fit}(L \cup U, Y, w)$ 
  return  $g$ 
end

```

Algorithm 1: Self-labeling grey-box learning algorithm with confidence amending.

It is important to mention that the black-box classifier should be able to measure calibrated probabilities in order to correctly interpret them as

the confidence of its predictions. Not all machine learning models are able to provide probabilities that match with the expected distribution of probabilities for each class. According to a study on different supervised classifiers regarding probabilities estimation [48], logistic regression, multilayer perceptrons and bagged trees naturally provide well calibrated probabilities, whereas others such as boosted trees and SVM produce distorted ones. When the calibration of probabilities is needed, two main options are available: Platt’s scaling [53] and isotonic regression [69]. Platt’s scaling is more recommended when the distortion in the predicted probabilities has a sigmoid shape, whereas isotonic regression is able to correct any monotonic distortion but it requires large amounts of data for avoiding overfitting.

4.2 Using the inclusion degree measures from Rough Set Theory

In this subsection we describe a second strategy for amending the enlarged dataset, which is based on the knowledge structures attached to Rough Set Theory [51]. This formalism allows handling uncertainty in the form of inconsistency through the computation of the lower and upper approximations for any set of instances in the decision space. The rough regions associated to these approximations can be used to weight the instances after performing the self-labeling process. Particularly, we assign higher weights to more confident instances as they have more chance to be correctly classified by the base black box.

4.2.1 Rough Set Theory

Rough Set Theory (RST) [51] is a mathematical formalism for handling uncertainty in the form of inconsistency in real-world applications. Given a decision system $DS = (\mathcal{U}, A \cup \{d\})$ where the universe of instances \mathcal{U} is described by a non-empty finite set of attributes A and its respective decision class d , any concept (subset of instances) $X \in \mathcal{U}$ can be approximated by two crisp sets. These sets are called lower and upper approximations of X ($\underline{B}X$ and $\overline{B}X$, respectively) and can be computed taking into account an equivalence relation, as follows:

$$\underline{B}X = \{x \in \mathcal{U} \mid [x]_B \subseteq X\} \quad (3)$$

$$\overline{B}X = \{x \in \mathcal{U} \mid [x]_B \cap X \neq \emptyset\} \quad (4)$$

The equivalence class $[x]_B$ gathers the instances in the universe \mathcal{U} which are inseparable according to a subset of attributes $B \subseteq A$. From the formulations of upper and lower approximation, we can derive the positive, negative and boundary regions of any subset $X \in \mathcal{U}$. The positive region $\mathcal{P}(X) = \underline{B}X$ includes those instances that are surely contained in X ; the negative region $\mathcal{N}(X) = \mathcal{U} - \overline{B}X$ denotes those instances that are surely not contained in X ,

while the boundary region $\mathcal{B}(X) = \overline{BX} - \underline{BX}$ captures the instances whose membership to the set X is uncertain, i.e., they might be members of X .

The classic RST is regularly defined over a subset of discrete attributes, thus generating a partition of \mathcal{U} . A more relaxed formulation of RST establishes the inseparability between instances based on a weak binary relation. Equation (5) formalizes the similarity relation used in this paper, which define whether any pair of instances x_i and x_j can be considered similar,

$$\mathcal{R} : x_i \mathcal{R} x_j \rightarrow \delta(x_i, x_j) \geq \varepsilon \quad (5)$$

where $\delta(x_i, x_j)$ computes the extent to which x_i and x_j are deemed inseparable as indicated by the similarity threshold ε . Under this assumption, the universe is arranged in similarity classes that are not longer disjoint but overlapped. In this paper, $\varepsilon = 0.98$ and the inseparability relation is defined as the complement of a distance function, such as the Heterogeneous Euclidean-Overlap Metric [62]. This distance function computes the normalized Euclidean distance between numerical attributes and an overlap metric for nominal attributes. Equations (6) and (7) define this dissimilarity function,

$$\delta(x_i, x_j) = \sqrt{\frac{\sum_{t=1}^{|B|} \omega_t \rho_t(x_i, x_j)}{\sum_{t=1}^{|B|} \omega_t}} \quad (6)$$

with,

$$\rho_t(x_i, x_j) = \begin{cases} 0 & \text{if } b_t \text{ is nominal} \wedge x_i(t) = x_j(t) \\ 1 & \text{if } b_t \text{ is nominal} \wedge x_i(t) \neq x_j(t) \\ (x_i(t) - x_j(t))^2 & \text{if } b_t \text{ is numerical} \end{cases} \quad (7)$$

where $x_i(t)$ and $x_j(t)$ denote the normalized values of the t -th attribute for heterogeneous instances x_i and x_j , respectively, and ω_t is the information gain of the b_t attribute.

Once the covering of the decision space is generated according to the similarity function, several RST based measures can be computed for measuring the uncertainty contained in a dataset [2]. In the following subsection, we adopt one of these measures to weight the instances belonging to the enlarged training set obtained after performing the self-labeling process.

4.2.2 Inclusion degree

The use of this amending strategy is based on the fact that the black box could produce wrong labels for unlabeled instances. In addition, there is no guarantee that the knowledge concerning the original labeled instances is confident. To address both situations together, we propose a mechanism to weight the instances after the self-labeling process. Unlike the confidence-based strategy, this amending procedure is adopted for the entire enlarged dataset, instead of

only the self-labeled instances. Therefore, it treats the uncertainty in the form of inconsistency of the labeled and unlabeled instances together.

More explicitly, the second weighting strategy is based on the inclusion degree of both labeled and self-labeled instances into the RST granules, thus let $X = L \cup U$ and $d = y$. Let $\mu_{\mathcal{P}(y_i)}^{\mathcal{R}}(x)$, $\mu_{\mathcal{B}(y_i)}^{\mathcal{R}}(x)$ and $\mu_{\mathcal{N}(y_i)}^{\mathcal{R}}(x)$ denote the membership degrees of any instance x to the positive, boundary and negative region of each class label y_i , respectively. These membership degrees are computed from the inclusion degree of the similarity class of x into each information granule,

$$\mu_{\mathcal{P}(y_i)}^{\mathcal{R}}(x) = \frac{|\bar{\mathcal{R}}(x) \cap \mathcal{P}(X_{[y_i]})|}{|\mathcal{P}(X_{[y_i]})|} \quad (8)$$

$$\mu_{\mathcal{B}(y_i)}^{\mathcal{R}}(x) = \frac{|\bar{\mathcal{R}}(x) \cap \mathcal{B}(X_{[y_i]})|}{|\mathcal{B}(X_{[y_i]})|} \quad (9)$$

$$\mu_{\mathcal{N}(y_i)}^{\mathcal{R}}(x) = \frac{|\bar{\mathcal{R}}(x) \cap \mathcal{N}(X_{[y_i]})|}{|\mathcal{N}(X_{[y_i]})|} \quad (10)$$

where $\bar{\mathcal{R}}(x)$ is the similarity class associated with the instance x , whereas $X_{[y_i]}$ denotes the set of instances with label y_i .

Equation (11) computes the weight for the instance x belonging to the enlarged dataset, given its label y_i and a similarity relation \mathcal{R} . The sigmoid function $\varphi(\cdot)$ is used to maintain the weight in the $(0, 1)$ range.

$$w_{(x,y_i)} = \varphi \left(\mu_{\mathcal{P}(y_i)}^{\mathcal{R}}(x) + 0.5 * \mu_{\mathcal{B}(y_i)}^{\mathcal{R}}(x) - \mu_{\mathcal{N}(y_i)}^{\mathcal{R}}(x) \right) \quad (11)$$

Observe that the boundary information is also interesting, since a high inclusion degree of an instance in the boundary region of a class is to some extent a positive evidence. This knowledge can be reinforced or diluted according to the evidence coming from the inclusion degrees in the other two regions. When using the RST based amending, Equation (11) replaces Equation (2) in the pseudocode of Algorithm 1.

Figure 2 illustrates the inclusion of the amending procedures into the learning algorithm of the SIGb approach. It is important to note that the amending process is only carried out in the learning phase of the self-labeling grey-box. Therefore, the amending strategies do not affect the transparency of the white-box surrogate during the inference on new cases.

However, the use of amending by weighting has implications for the interpretability, since assigning high weights to a small subset of instances transforms the global surrogate model toward a rather local one. Weighting instances makes the white-box surrogate biased toward learning from the most confident examples, therefore it would mostly provide explanations for that particular subspace of the domain. However, it makes sense to prioritize interpretability or explanations over the predictions that are most certain in the problem domain.

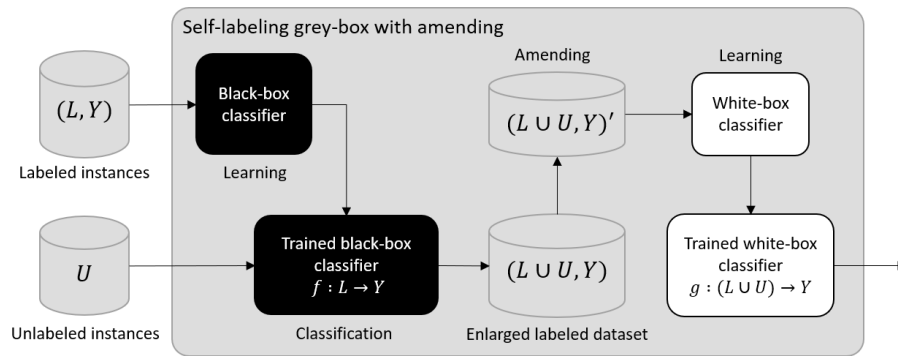


Fig. 2: Architecture of the SIGb approach using amending procedures. The enlarged dataset is weighted using calibrated probabilities or RST inclusion degree.

5 Experiments and discussion

In this section, we evaluate the SIGb approach through a three-step methodology using standard benchmark datasets. Unlike other experiments reported in the literature, the one developed in this section evaluates both algorithms' performance and interpretability, when having different percentages of labeled instances. As a complement, we propose three new evaluation measures that go beyond the prediction rates.

Being more specific, the *first step* of our experimentation methodology is devoted to determining which black-box classifier produces the best results in terms of prediction performance. This step is quite important since the overall performance will depend on the discriminatory ability of the black box. The *second step* is dedicated to determining which combination of white box and amending reaches the best commitment between prediction rates and interpretability. As a *third step*, we further explore the impact of having different percentages of labeled and unlabeled instances on the algorithm's performance.

As a complement of the evaluation methodology for interpretable SSC methods, in the last part of this section we compare SIGb against the best-performing state-of-the-art methods. In this case, the evaluation is confined to the prediction rates as these methods cannot be interpreted, thus the goal here is to show that SIGb is not just simple and elegant, but also able to outperform other self-labeling methods reported in the literature.

5.1 Benchmark datasets, base classifiers and parameter settings

Our experimental design includes 55 challenging and diverse datasets. Four ratios of labeled instances in the training set (from 10% to 40%) allow studying the influence of the amount of labeled examples in the overall perfor-

mance. These datasets comprise different characteristics: the number of instances ranges from 100 to 19000, the number of attributes from 2 to 90, and the number of decision classes from 2 to 28. Moreover, we have 25 datasets with different degrees of class imbalance and roughly half of the datasets are multiclass problems (see Table 1).

These datasets are partitioned into training and test sets as done in a 10-fold cross-validation, so each training set consists in labeled and unlabeled instances. The subset of unlabeled instances is obtained by performing a random selection without replacement and neglecting the class label of such instances. These datasets (including the cross-validation fold partitions) were provided as a supplementary material in [57].

There are several algorithms that can be adopted as base classifiers. On the one hand, the selected classifier for the base black box should exhibit a strong predictive capability as it is used to determine the decision class of unlabeled instances. Following, we describe three mainstream supervised classifiers that will be used in the experiments for instantiating the black-box component. Several studies provide experimental evidence of their superior performance in a wide range of classification problems [70, 21, 59]. In addition, when the amending through confidence is used, the black box is subject to one restriction: it should be able to measure calibrated probabilities of membership to each class. As previously mentioned, different alternatives are available for dealing with this issue.

Black-box classifiers

- Random Forests (RF) [8]: Bagging of random trees. Composed of decision trees without pruning that consider m randomly chosen attributes at each node. Hyperparameters: 100 trees, number of random attributes to select: $\log_2(\text{attributes}) + 1$.
- Multilayer Perceptron (MLP) [35]: Feed-Forward Neural Network with backpropagation algorithm. Hyperparameters: learning rate: 0.3, momentum: 0.2, learning iterations: 500, number of hidden layers: 1, number of neurons: $(\text{attributes} + \text{classes})/2$.
- Support Vector Machine (SVM) [39]: Support vector classifier using John Platt’s sequential minimal optimization algorithm for training. Hyperparameters: kernel: polynomial kernel. Uses Platt’s Scaling for the calibration of probabilities [12].

On the other hand, for the white-box component any classifier that can act as a surrogate model for interpretability can be used. Therefore, the choice of a white box must be driven by the type of interpretability that is needed. Additionally, it must be able to handle weighted instances in the learning process. Next we describe three classifiers explored in the scope of this paper:

White-box classifiers

- Decision Tree (C45) [54]: Induces rules in the form of a pruned decision tree using C4.5 algorithm. Hyperparameters: minimum number of objects per

Table 1: Characterization of the datasets used in the experiment.

Dataset	Instances	10%	20%	30%	40%	Features	Classes
abalone	4174	417	835	1252	1670	8	28
appendicitis	106	11	21	32	42	7	2
australian	690	69	138	207	276	14	2
autos	205	21	41	62	82	25	6
banana	5300	530	1060	1590	2120	2	2
breast	286	29	57	86	114	9	2
bupa	345	35	69	104	138	6	2
chess	3196	320	639	959	1278	36	2
cleveland	297	30	59	89	119	13	5
coil2000	9822	982	1964	2947	3929	85	2
contraceptive	1473	147	295	442	589	9	3
crx	125	13	25	38	50	15	2
dermatology	366	37	73	110	146	33	6
ecoli	336	34	67	101	134	7	8
flare-solar	1066	107	213	320	426	9	6
german	1000	100	200	300	400	20	2
glass	214	21	43	64	86	9	7
haberman	306	31	61	92	122	3	2
heart	270	27	54	81	108	13	2
hepatitis	155	16	31	47	62	19	2
housevotes	435	44	87	131	174	16	2
iris	150	15	30	45	60	4	3
led7digit	500	50	100	150	200	7	10
lymphography	148	15	30	44	59	18	4
magic	19020	1902	3804	5706	7608	10	2
mammographic	961	96	192	288	384	5	2
marketing	8993	899	1799	2698	3597	13	9
monks	432	43	86	130	173	6	2
movement_libras	360	36	72	108	144	90	15
mushroom	8124	812	1625	2437	3250	22	2
nursery	12690	1269	2538	3807	5076	8	5
pageblocks	5472	547	1094	1642	2189	10	5
penbased	10992	1099	2198	3298	4397	16	10
phoneme	5404	540	1081	1621	2162	5	2
pima	768	77	154	230	307	8	2
ring	7400	740	1480	2220	2960	20	2
saheart	462	46	92	139	185	9	2
satimage	6435	644	1287	1931	2574	36	7
segment	2310	231	462	693	924	19	7
sonar	208	21	42	62	83	60	2
spambase	4597	460	919	1379	1839	55	2
spectheart	267	27	53	80	107	44	2
splice	3190	319	638	957	1276	60	3
tae	151	15	30	45	60	5	3
texture	5500	550	1100	1650	2200	40	11
tic-tac-toe	958	96	192	287	383	9	2
thyroid	7200	720	1440	2160	2880	21	3
titanic	2201	220	440	660	880	3	2
twonorm	7400	740	1480	2220	2960	20	2
vehicle	846	85	169	254	338	18	4
vowel	990	99	198	297	396	13	11
wine	178	18	36	53	71	13	3
wisconsin	683	68	137	205	273	9	2
yeast	1484	148	297	445	594	8	10
zoo	101	10	20	30	40	17	7

- leaf: 2, confidence factor for pruning: 0.25, uses subtree raising operation when pruning.
- PART Decision List (PART) [22]: Decision list using separate-and-conquer for building rules. Generates a partial C4.5 decision tree in each iteration and makes the "best" leaf into a rule. Hyperparameters: minimum number of objects per leaf: 2, confidence factor for pruning: 0.25, uses subtree raising operation when pruning.
 - RIPPER Decision List (RIP) [15]: Propositional rule learner based in association rules with reduced error pruning. The training data is split into a growing set and a pruning set. The rule set formed from the growing set is simplified by pruning operators such as it yields the greatest reduction of error on the pruning set. Hyperparameters: minimum total weight of instances in a rule: 2.0, number of folds: 3 (1 for pruning), number of optimizations: 2.

Amending procedures

- No amending (NONE): Not using amending, all self-labeled instances are provided as extra data to the surrogate white box. Used as baseline for estimating the contribution of the two amending procedures described in this paper.
- Calibrated probabilities based amending (CONF): Amending procedure described in subsection 4.1.
- RST inclusion degree based amending (RST): Amending procedure described in subsection 4.2.

Hereinafter, when referring to a particular configuration of our approach we denote it as "*bb-wb-am*" where *bb* is the base black box, *wb* is the surrogate white box and *am* is the amending procedure².

5.2 Determining the best-performing black-box component

We first focus on evaluating the influence of the base black box in the performance of the algorithm. Here no amending procedure is taken into account yet since it does not directly affects the ability of the black box to produce correct classifications. In order to measure the configurations in terms of prediction rates we report the Cohen's kappa coefficient [14]. This measure estimate the inter-rater agreement for categorical items and ranges in $[-1, 1]$, where -1 indicates no agreement between the prediction and the actual values, 0 means no learning (i.e., random prediction), and 1 total agreement or perfect performance. While accuracy is considered mainstream when measuring classification rates, the kappa is a more robust measure since this coefficient takes into account the agreement occurring by chance, which is especially relevant for datasets with class imbalance [37, 3].

² Code, datasets and results using different measures are provided as supplementary material for reproducibility purposes in gitlab.ai.vub.ac.be/igraugar/slgb_scripts/tree/paper

Table 2 gives the mean and the standard deviation of the kappa coefficient achieved on each setting. We group the results for different percentages of labeled instances. The numerical simulations indicate that using RF as the black-box component leads to higher prediction rates. In particular, the RF-PART-NONE configuration stands as the best performing one for varying amounts of labeled instances, very closely followed by RF-C45-NONE and RF-RIP-NONE.

Table 2: Prediction rates (kappa) achieved by different combinations of black-box and white-box algorithms without using amending. Results are grouped by ratio and best results are highlighted in bold.

	Ratio	10%	20%	30%	40%
MLP-C45-NONE	mean	0.50	0.53	0.55	0.56
	stdev	0.28	0.28	0.28	0.28
MLP-PART-NONE	mean	0.50	0.54	0.56	0.57
	stdev	0.29	0.28	0.28	0.28
MLP-RIP-NONE	mean	0.51	0.54	0.55	0.57
	stdev	0.29	0.28	0.28	0.28
RF-C45-NONE	mean	0.56	0.60	0.61	0.61
	stdev	0.28	0.27	0.27	0.27
RF-PART-NONE	mean	0.56	0.60	0.61	0.62
	stdev	0.29	0.27	0.27	0.27
RF-RIP-NONE	mean	0.55	0.60	0.61	0.62
	stdev	0.28	0.27	0.27	0.27
SVM-C45-NONE	mean	0.49	0.53	0.55	0.56
	stdev	0.28	0.27	0.27	0.26
SVM-PART-NONE	mean	0.50	0.53	0.56	0.57
	stdev	0.28	0.28	0.28	0.27
SVM-RIP-NONE	mean	0.50	0.53	0.55	0.57
	stdev	0.28	0.28	0.27	0.27

With the aim of providing a rigorous statistical analysis of the differences, we compute the Friedman two-way analysis of variances by ranks [23], per ratio. The test suggests rejecting the null hypotheses for all labeled ratios based on a confidence interval of 95% (see Table 6 in appendix³). This means that there exist significant differences between at least two configurations on each ratio. The next step is focused on determining whether RF black box is truly superior compared to other configurations. To do so, we adopt the Wilcoxon signed rank test [61] and Holm’s post-hoc procedure [36] to correct the p -values, as suggested by Benavoli *et al.* [4]. Table 7 reports the unadjusted p -value computed by the Wilcoxon test and the corrected p -value associated with each pairwise comparison. In order to discover the influence of the black box we compare the pairs of configurations using the same surrogate white box. Each section of the table represents the ratio of labeled instances. The null hypothesis states that there is no significant difference between the performance

³ All tables related to statistical tests are included in the appendix.

of each pair of configurations. All null hypotheses are rejected, except for RF-RIP vs. MLP-RIP in the 40% ratio (however RF still has higher prediction rates). This suggests that RF is clearly the best-performing base black box for the self-learning grey-box. This result is not surprising since RF has proven to be very competent classifier in different experimental studies [70, 21, 59, 56]. Furthermore, RF produces consistent probabilities that does not need to be calibrated [48], which is a requirement for the later use of confidence-based amending.

5.3 Impact of using different white boxes and amending configurations

In this section, we study how different choices of the amending processes and white-box surrogates impact the overall results. Therefore, we first explore the influence on the prediction rates. Based on the selection of RF as black-box base, Table 3 shows very similar results across each ratio. Going deeper with the statistical analysis, we apply Friedman and Wilcoxon tests with post-hoc correction. Although Friedman test finds significant differences in the four groups (Table 8), examining Wilcoxon corrected tests we ascertain that the null hypothesis cannot be rejected for the vast majority of pairs compared (see Table 9 for details). This means that there are no statistically significant differences in the prediction rates when comparing different amending procedures with a fixed white box and vice versa. This behavior suggests that the overall prediction rates of the approach mostly relies on the correct choice of the black-box algorithm.

Table 3: Prediction rates achieved by different combinations of white boxes and amending strategies while using RF as black box. Results are grouped by ratio and best results are highlighted in bold.

	Ratio	10%	20%	30%	40%
RF-C45-NONE	mean	0.56	0.60	0.61	0.61
	stdev	0.28	0.27	0.27	0.27
RF-PART-NONE	mean	0.56	0.60	0.61	0.62
	stdev	0.28	0.27	0.27	0.27
RF-RIP-NONE	mean	0.55	0.60	0.61	0.62
	stdev	0.28	0.27	0.27	0.27
RF-C45-CONF	mean	0.55	0.59	0.61	0.61
	stdev	0.29	0.28	0.28	0.28
RF-PART-CONF	mean	0.56	0.60	0.61	0.62
	stdev	0.29	0.27	0.27	0.27
RF-RIP-CONF	mean	0.54	0.59	0.61	0.60
	stdev	0.29	0.27	0.27	0.28
RF-C45-RST	mean	0.56	0.60	0.62	0.62
	stdev	0.29	0.27	0.27	0.28
RF-PART-RST	mean	0.56	0.61	0.62	0.62
	stdev	0.28	0.27	0.27	0.27
RF-RIP-RST	mean	0.53	0.57	0.58	0.59
	stdev	0.28	0.28	0.28	0.28

However, when examining the number of rules obtained, the difference is significantly visible. Figure 3 plots of the number of rules produced by each combination, per ratio of labeled data. Two results are consistent across ratios: both amending strategies (specially RST) reduce the number of rules while RIP as surrogate white box produces the lowest number of rules for all possible combinations.

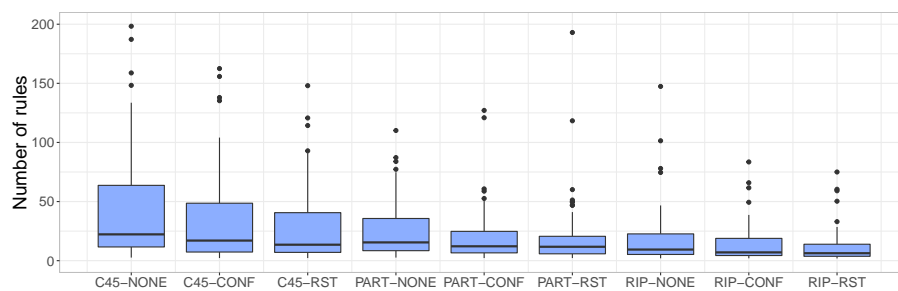
Toward exploring this result further, we also propose two new measures to evaluate models' interpretability via a quantifiable proxy. The first measure can be used in the context of self-labeling and the second one is applicable to any model containing explanation units. According to [17], there are three main forms of evaluating interpretability: application-grounded, human-grounded and functionally-grounded metrics. The functionally-grounded approach is the only one not requiring human experiments and collaboration. As an alternative it uses desiderata for interpretability (e.g. transparency, trust, etc.) as a proxy for assessing the quality of the model. Although this form of evaluation is the most commonly found in literature, the proposed measures are predominantly related to the context of fuzzy rule-based systems [9, 25] focusing on the number of rules or fuzzy regions. Since we are working with benchmark datasets, we use the functionally-grounded approach for creating measures based on the simplicity as a mean for gaining transparency and simulatability (i.e. a human is able to simulate and reason about the model's entire decision-making process). The first measure can be used in the context of self-labeling for base methods that produce tree structures, rules or decision lists. It involves the number of rules in the decision lists (or equivalently the number of leaves in a decision tree) and expresses the *relative growth* in structure as:

$$\Gamma = |E^g|/|E^w| \quad (12)$$

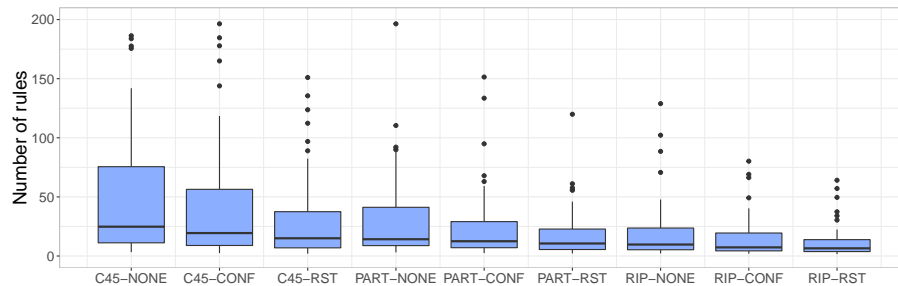
where E^g is the set of rules produced by the self-labeling method (here the grey-box) and E^w is the set of rules produced by the baseline white box when using only labeled data. For this measure, a number much greater than one indicates that a major growth in the structure of the self-labeling method is needed when using the extra unlabeled data. In that case, the balance between interpretability and performance must be taken into account for further evaluation.

The second measure is more general and applicable to any model whose structure is formed by quantifiable explanation units (e.g. rules, prototypes, features, derived features, etc.). Here, this measure estimates the *simplicity* of the model according with the size of the structure in terms of number of rules. Although it is often presumed that the smaller the rule set the better, this is not necessarily a linear relation. The desired simplicity in terms of number of rules has a smooth behaviour which can drop quickly. Therefore, we propose to measure simplicity through a generalized sigmoid function, since it allows to represent this relation with enough flexibility:

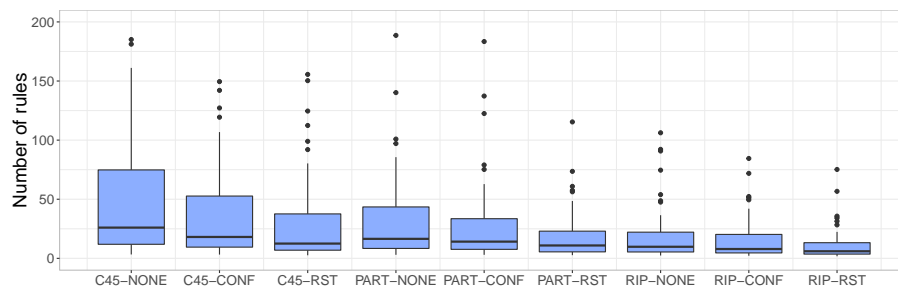
$$\Upsilon(|E^g|) = \phi(|E^g|, \theta_1, \theta_2, \lambda, \eta, \nu) \quad (13)$$



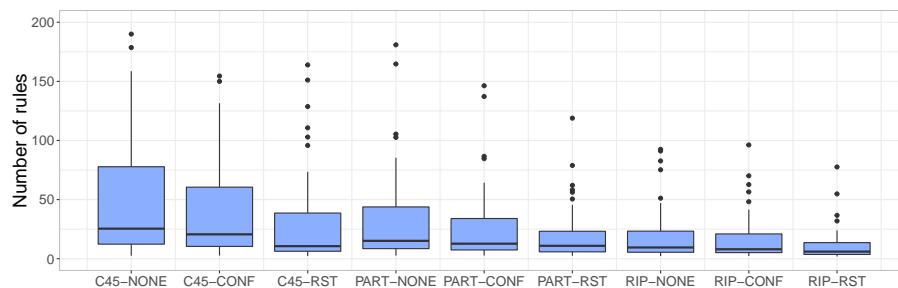
(a) Using 10% of labeled instances.



(b) Using 20% of labeled instances.



(c) Using 30% of labeled instances.



(d) Using 40% of labeled instances.

Fig. 3: Number of rules produced by each combination of white box and amending, using random forests as black box. Both amending strategies (specially RST) reduce the number of rules while RIP white box produces the lowest number of rules.

$$\phi(|E^g|, \theta_1, \theta_2, \lambda, \eta, \nu) = \theta_1 + \frac{\theta_2 - \theta_1}{(1 + e^{-\lambda(|E^g| - \eta)})^{1/\nu}} \quad (14)$$

where $\theta_1 = 1$ and $\theta_2 = 0$ represent the upper and lower asymptotes of the function respectively, λ is the slope of the curve, η regulates the shift over the x -axis and ν affects near which asymptote maximum growth occurs. In this way, a value of 1 indicates high simplicity and it decreases smoothly toward 0. A bigger λ would make the function less smooth and the value of η moves where the middle value of the function is obtained. A value of $\nu = 1$ makes no change in the curve, while $\nu < 1$ moves the growth toward the upper asymptote and $\nu > 1$ toward the lower one. Observe that both η and ν influence where 0.5 simplicity is obtained. In real application scenarios these parameters should be decided based on the criteria of domain experts. Given the diversity of our benchmark data, we take $\lambda = 0.1, \eta = 30, \nu = 0.5$ for illustrating a general setting (see Fig. 4).

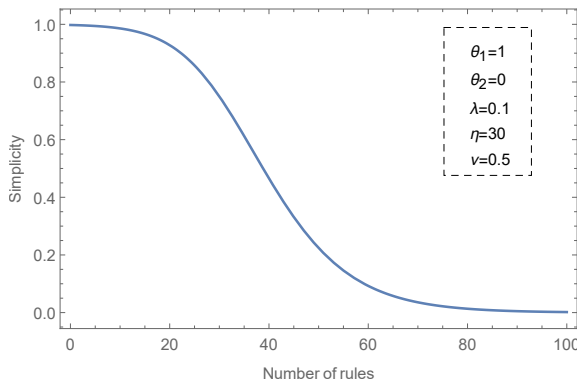


Fig. 4: Simplicity function with default parameters used for the benchmark datasets. For specific applications these parameters are domain dependant.

With these values, the function produces medium evaluations (around 0.5) when the number of rules is around 40. Similarly, it obtains rather high simplicity (higher than 0.8) when the number of rules goes below 30. However, parameter values should be estimated based on expert knowledge for specific applications. This highly flexible function allows customizing the value of simplicity according with the specifics of a given case study.

Table 4 shows the average relative growth and simplicity over the 55 datasets tested for the four ratios. Regarding the relative growth, the increase in the structure of the grey-box is on average larger when using small amounts of labeled data, while for bigger ratios this difference decreases. This growth in the structure is an expected consequence of providing more unlabeled data to the white-box surrogate in the grey-box scheme. However, the use of amending procedures alleviates this effect by giving more importance to relevant

unlabeled instances. In general, a smaller growth is observed when using RST amending, especially in combination with PART as the white box, thus resulting in the winner combination for all ratios.

Table 4: Mean (and standard deviation) of the relative growth and simplicity achieved by different combinations of white boxes and amending strategies while using RF as black box. Results are grouped by ratio and best results are highlighted in bold.

	Ratio	10%	20%	30%	40%
RF-C45-NONE	growth	4.24 (2.98)	3.22 (3.81)	3.00 (6.61)	3.95 (15.12)
	simplicity	0.57 (0.44)	0.56 (0.45)	0.56 (0.45)	0.56 (0.45)
RF-PART-NONE	growth	3.07 (0.92)	2.19 (0.62)	1.78 (0.51)	1.55 (0.47)
	simplicity	0.70 (0.39)	0.70 (0.39)	0.69 (0.40)	0.69 (0.40)
RF-RIP-NONE	growth	3.93 (4.78)	3.19 (4.13)	2.93 (4.48)	2.67 (4.37)
	simplicity	0.85 (0.28)	0.84 (0.29)	0.84 (0.30)	0.84 (0.30)
RF-C45-CONF	growth	2.74 (2.38)	2.34 (3.35)	2.43 (5.96)	3.39 (13.75)
	simplicity	0.67 (0.42)	0.63 (0.44)	0.61 (0.45)	0.60 (0.45)
RF-PART-CONF	growth	2.11 (0.59)	1.66 (0.47)	1.45 (0.43)	1.30 (0.40)
	simplicity	0.81 (0.32)	0.78 (0.34)	0.75 (0.35)	0.74 (0.36)
RF-RIP-CONF	growth	2.96 (2.94)	2.52 (3.17)	2.41 (3.94)	2.54 (5.87)
	simplicity	0.89 (0.39)	0.88 (0.25)	0.87 (0.26)	0.86 (0.27)
RF-C45-RST	growth	2.26 (0.93)	1.53 (0.61)	1.20 (0.59)	1.00 (0.33)
	simplicity	0.71 (0.39)	0.71 (0.39)	0.71 (0.39)	0.71 (0.40)
RF-PART-RST	growth	1.99 (0.49)	1.38 (0.31)	1.13 (0.24)	0.98 (0.21)
	simplicity	0.82 (0.32)	0.81 (0.33)	0.81 (0.33)	0.81 (0.34)
RF-RIP-RST	growth	2.42 (2.26)	1.69 (1.06)	1.39 (0.63)	1.20 (0.42)
	simplicity	0.91 (0.23)	0.92 (0.21)	0.93 (0.19)	0.94 (0.18)

In addition, the simplicity measure (the closer the value to one the better) also indicates that the use of amending is convenient for obtaining more concise sets of rules. It is also evident that using RIP as surrogate generates the least number of rules, followed by PART. For this measure the absolute winner is RF-RIP-RST combination, exhibiting the highest values of simplicity for all ratio values used for experimentation. A similar statistical validation support this statement (see tables 10 and 11), finding significant statistical differences when comparing RF-RIP-RST with other configurations using simplicity as interpretability measure.

It is important to remark that the simplicity measure solely expresses what it would be considered a manageable model. Of course, a very simple model with only one rule and poor prediction rates is not desirable, whereas for a very simple dataset it might happen that three or four rules are enough to reach accurate results. That is why taking into account the prediction performance is fundamental for a proper assessment. In order to measure algorithms' quality based on the balance between the prediction rates and the simplicity of the learned model, we propose a third measure — called *utility* — combining the kappa and the simplicity values with a mixing parameter α ,

$$\Psi(E^g) = \alpha * \kappa(E^g) + (1 - \alpha) * \Upsilon(|E^g|) \quad (15)$$

where α is set to 0.6 in our experimental setting.

As a partial summary, Fig. 5 visualizes the utility values in a heat-map plot. From this figure, it is easy to perceive that the RIP algorithm, as a white-box surrogate, positively contributes to the overall performance of the approach when taking both kappa and simplicity into account. Additionally, RST amending also increases the value of utility when compared with CONF amending or not using amending at all. This measure reflects that, in general, the best trade-off is reached when using the RF-RIP-RST combination and the highest values are achieved when more labeled data is available.

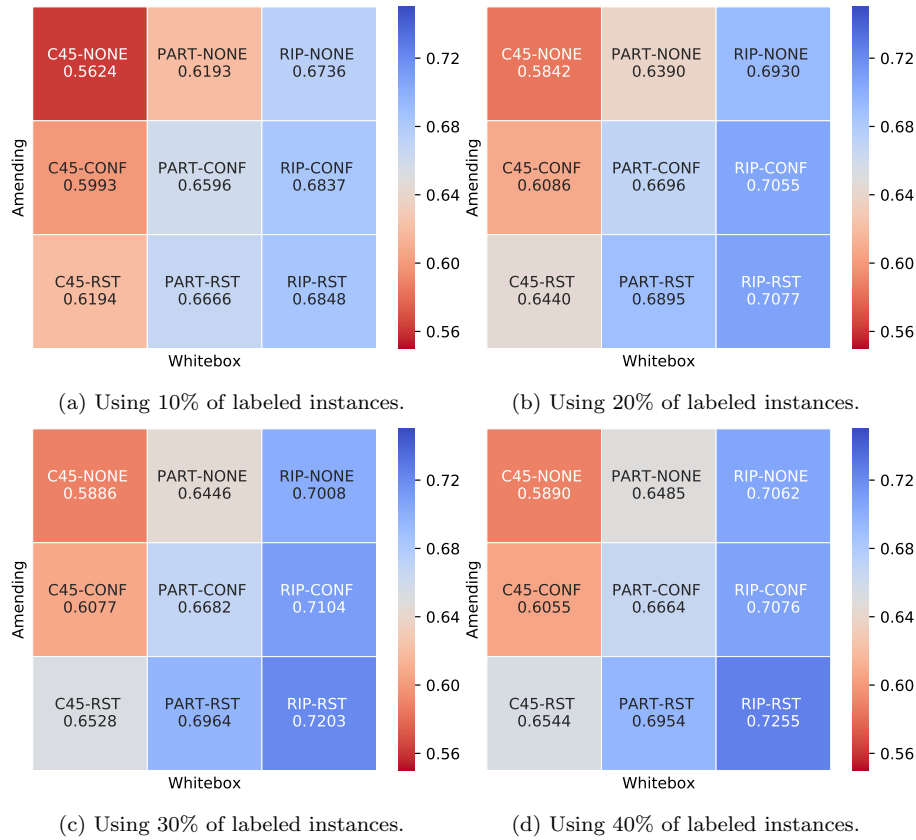


Fig. 5: Mean utility values of each combination of white box and amending, using random forests as the black-box base classifier.

5.4 Influence of the number of labeled and unlabeled instances

In this subsection, we use RF-RIP-RST to explore the impact of having different amounts of labeled and unlabeled instances on algorithm’s results. In the evaluation of semi-supervised techniques, it is a common strategy to vary the size of L by systematically neglecting the label of different amounts of instances and adding them to U . But this procedure does not explore the scenario where also the unlabeled instances could be hard to obtain [50]. Observe that since this is a controlled experiment we can safely assume that the unlabeled instances follow the same class distribution as the labeled ones. In reality, one might need to re-balance the dataset after self-labeling if the unlabeled instances per-class distribution significantly differs.

Due to the fact that we do not have truly unlabeled instances, we use the same datasets from the previous experiment. First, a test set with 20% of instances is kept aside for evaluation. Then, we divide the train set into two equally sized and disjoint subsets (each with 40% of the total instances). Each subset is a source for labeled and unlabeled instances, respectively, from where we vary the amount of instances we use for training. Figure 6 shows the surfaces resulting from the average of different measures over the 55 datasets.

From the first two surfaces Fig. 6a and 6b, it can be observed that the prediction rates (accuracy and kappa) have a pronounced increment when adding more labeled and unlabeled instances. Especially when labeled instances are very limited, the number of unlabeled instances seems to increase the performance. This result confirms that our approach fulfills the main hypothesis attached with self-labeling SSC approaches. In addition, the number of rules (Fig. 6c) increases almost linearly with the number of training instances. Although, the relative growth (Fig. 6d) is more sensitive to adding unlabeled data when labeled data is very scarce, i.e. a huge amount of unlabeled instances rapidly increases the structure and loses in interpretability, compared with the baseline white box. In addition, the simplicity (Fig. 6e) shows the expected behavior: the best values of this measure are observed with the least number of instances and it decreases uniformly in both directions. Finally, the utility surface (Fig. 6f) summarizes all results reflecting the increase in the overall performance when adding both labeled and unlabeled instances.

5.5 Comparing against state-of-the-art self-labeling classifiers

In this section we compare the predictive capability of SIGb against the four best self-labeling techniques reported in the review paper in [57]: Co-training using support vector machine [33] (CT(SMO)), Tri-training using C45 decision tree [72] (TT(C45)), Co-Bagging using C45 decision tree [33] (CB(C45)) and Democratic Co-learning [71] (DCT). Since these algorithms are not inherently interpretable we focus our comparison on the prediction rates only. For this section, SIGb refers to the RF-PART-RST combination which exhibits the best results in kappa, as showed in Subsection 5.3.

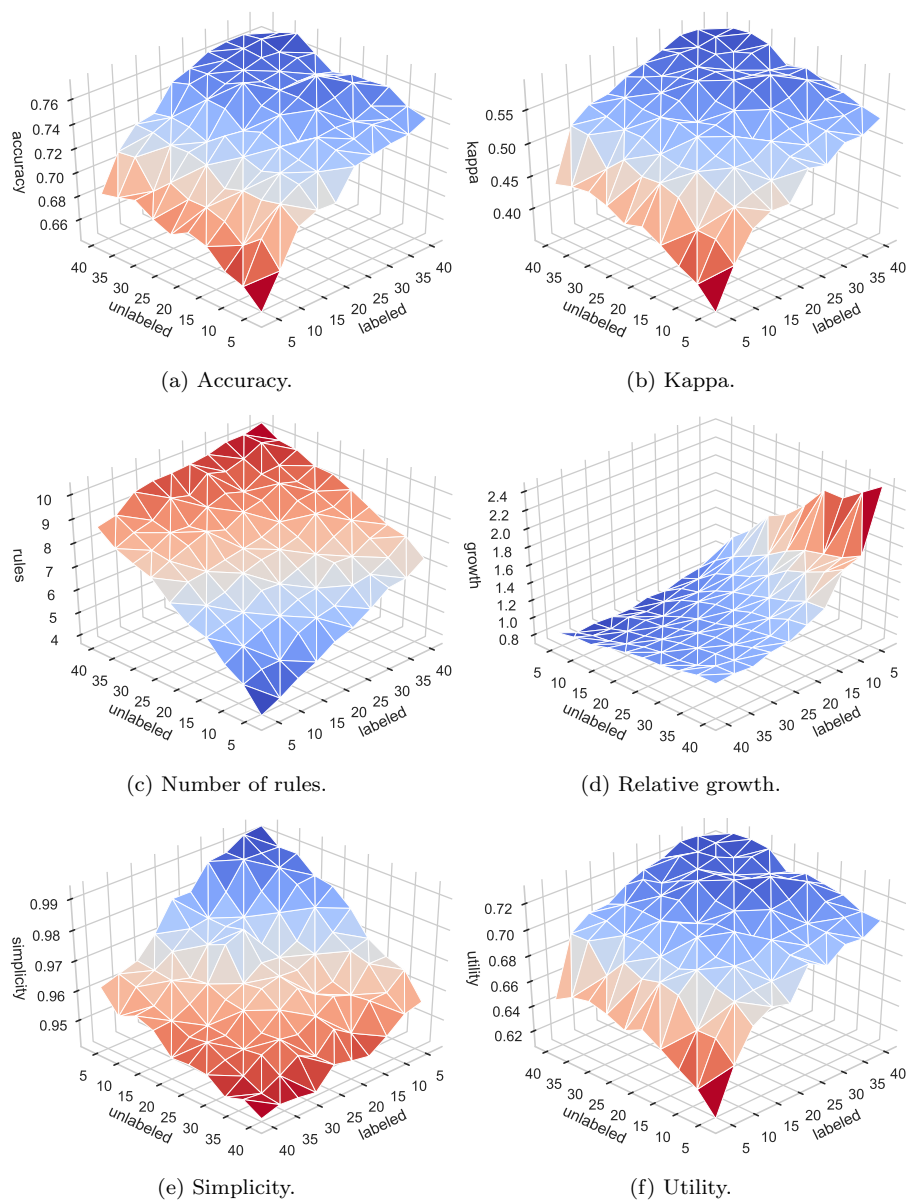


Fig. 6: Performance of RF-RIP-RST when varying the number of labeled and unlabeled instances, for different measures. Axes x and y are expressed in percentage of instances taken for training from each subset. Sub-figures (d) and (e) are rotated for visualization purposes.

Table 5 reports the mean and standard deviation of kappa coefficient for each classifier, taking into account the four studied ratios. The results reveal that SIGb has the highest mean for all ratios. In order to support this assertion, we compute the Friedman p -value per ratio. The test suggests rejecting the null hypotheses for all labeled ratios based on a confidence interval of 95% (see Table 12). This means that there is an indication that there exist significant differences between at least two algorithms in each comparison.

Table 5: Mean and standard deviation of kappa coefficient obtained by SIGb and four self-labeling methods from the state-of-the-art. The best performance is highlighted in bold.

	10%		20%		30%		40%	
	mean	stdev	mean	stdev	mean	stdev	mean	stdev
SIGb	0.56	0.29	0.61	0.27	0.62	0.27	0.62	0.27
TT(C45)	0.51	0.29	0.55	0.29	0.57	0.29	0.59	0.29
CB(C45)	0.51	0.29	0.55	0.29	0.57	0.29	0.56	0.28
DCT	0.49	0.32	0.54	0.30	0.58	0.28	0.59	0.28
CT(SMO)	0.48	0.31	0.55	0.29	0.58	0.29	0.60	0.29

The next step is focused on determining whether the superiority of the SIGb classifier is responsible for the significant difference reported by the Friedman test. Similar to previous sections we use the Wilcoxon signed rank test and the Holm post-hoc procedure for computing the corrected p -values associated with each pairwise comparison. Each section of the Table 13 represents a ratio of labeled instances. The null hypothesis states that there is no significant difference between the performance of each pair of algorithms, taking SIGb as the control one.

From the statistical tests we can draw the following conclusions. First, there is no doubt about the superiority of the SIGb classifier when tested with datasets with ratios of 10% and 20% of labeled instances, as all the null hypotheses were rejected. This result, in combination with the first place in the Friedman ranking, demonstrates that our algorithm significantly outperforms the other four algorithms in these settings. In the case of datasets comprising 30% and 40% of labeled instances, the results show that SIGb is the best-performing classifier, but with no significant differences observed between the pairs SIGb vs. DCT (for 30%), and SIGb vs. CT(SMO) (for both ratios), as these null hypotheses could not be rejected. However, DCT and CT(SMO) cannot be considered transparent due to their complex structure involving support vector machines and collaboration between base classifiers. Although our main goal was not to outperform the SSC methods in terms of classification rates, the analysis reported above supports our claim that we obtain a favorable balance between performance and interpretability by using the self-labeling grey-box approach for solving SSC problems.

6 Conclusions

In this paper, we report on an extended experimental study to determine the suitability of self-labeling grey-box classifier for semi-supervised classification problems where interpretability is a requirement. We explore two different amending procedures for weighting the instances coming from the self-labeling process. Such procedures aim at preventing the effect of misclassifications to propagate across the whole model. The experiments have shown that using Random Forests as the base black box for the self-labeling process is the best choice in terms of prediction rates. The choice of a white box and amending does not significantly affect the prediction rates but it is relevant for the size of the structure. Decision lists as surrogate white boxes produce less number of rules than the C4.5 decision tree, even when no amending is used. However, amending produces further decrease the size of the structure without affecting the prediction rates by giving more importance to confident instances in the self-labeling. Especially RST based amending looks more promising since it does not need the black-box base classifier to provide calibrated probabilities. Furthermore, RST based amending could be a good choice for a given case study where the uncertainty coming from inconsistency is high, even on the available labeled data. Therefore, we strongly advise the use of Random Forests as base black box and RST for amending the self-labeling, while the choice of white box is more flexible to the desired outcome, either a decision tree with rules or a decision list. In addition, the experimental comparison shows that our SIGb is able to outperform the best state-of-the-art self-labeling approaches across a standard benchmark of SSC datasets, yet being far more simple in structure than these techniques.

References

1. Albinati J, Oliveira SEL, Otero FEB, Pappa GL (2015) An ant colony-based semi-supervised approach for learning classification rules. *Swarm Intelligence* 9(4):315–341
2. Bello R, Verdegay JL (2012) Rough sets in the Soft Computing environment. *Information Sciences* 212:1–14
3. Ben-David A (2008) Comparison of classification accuracy using cohens weighted kappa. *Expert Systems with Applications* 34(2):825–832
4. Benavoli A, Corani G, Mangili F (2016) Should we really use post-hoc tests based on mean-ranks? *Journal of Machine Learning Research* 17:1–10
5. Bennett KP, Demiriz A (1999) Semi-supervised support vector machines. In: *Advances in Neural Information Processing Systems* 11, MIT Press, pp 368–374
6. Blum A, Chawla S (2001) Learning from labeled and unlabeled data using graph mincuts. In: *Proceedings of the Eighteenth International Conference on Machine Learning*, Morgan Kaufmann Publishers Inc., San Francisco, CA, USA, pp 19–26

7. Blum A, Mitchell T (1998) Combining labeled and unlabeled data with co-training. In: Proceedings of the Eleventh Annual Conference on Computational Learning Theory, ACM, New York, NY, USA, pp 92–100
8. Breiman L (2001) Random forests. *Machine Learning* 45(1):5–32
9. Cano A, Zafra A, Ventura S (2013) An interpretable classification rule mining algorithm. *Information Sciences* 240:1 – 20
10. Cevikalp H, Franc V (2017) Large-scale robust transductive support vector machines. *Neurocomputing* 235:199 – 209
11. Chakraborty S, Tomsett R, Raghavendra R, Harborne D, Alzantot M, Cerutti F, Srivastava M, Preece A, Julier S, Rao RM, et al. (2017) Interpretability of deep learning models: a survey of results. In: Proceedings of the IEEE Smart World Congress 2017
12. Chang CC, Lin CJ (2011) Libsvm: A library for support vector machines. *ACM Transactions on Intelligent Systems and Technology* 2(3):27:1–27:27
13. Chapelle O, Schlkopf B, Zien A (2010) *Semi-Supervised Learning*, 1st edn. The MIT Press
14. Cohen J (1960) A coefficient of agreement for nominal scales. *Educational and Psychological Measurement* 20(1):37–46
15. Cohen WW (1995) Fast effective rule induction. In: Friedlitis A, Russell S (eds) Proceedings of the Twelfth International Conference on Machine Learning, Morgan Kaufmann Publishers Inc., San Francisco, CA, USA, pp 115 – 123
16. Dai Z, Yang Z, Yang F, Cohen WW, Salakhutdinov RR (2017) Good semi-supervised learning that requires a bad GAN. In: Guyon I, Luxburg UV, Bengio S, Wallach H, Fergus R, Vishwanathan S, Garnett R (eds) Advances in Neural Information Processing Systems 30, Curran Associates, Inc., pp 6510–6520
17. Doshi-Velez F, Kim B (2018) Considerations for Evaluation and Generalization in Interpretable Machine Learning, Springer, pp 3–17
18. Fan M, Zhang X, Du L, Chen L, Tao D (2018) Semi-supervised learning through label propagation on geodesics. *IEEE Transactions on Cybernetics* 48(5):1486–1499
19. Fazakis N, Karlos S, Kotsiantis S, Sgarbas K (2015) Speaker identification using semi-supervised learning. In: Proceeding of the 2015 International Conference on Speech and Computer, Springer, vol LNCS 931, pp 389–396
20. Fazakis N, Karlos S, Kotsiantis S, Sgarbas K (2016) Self-trained LMT for semisupervised learning. *Computational Intelligence and Neuroscience* 2016:10
21. Fernández-Delgado M, Cernadas E, Barro S, Amorim D (2014) Do we need hundreds of classifiers to solve real world classification problems. *Journal of Machine Learning Research* 15(1):3133–3181
22. Frank E, Witten IH (1998) Generating accurate rule sets without global optimization. In: Proceedings of the Fifteenth International Conference on Machine Learning, Morgan Kaufmann Publishers Inc., San Francisco, CA, USA, pp 144–151

23. Friedman M (1937) The use of ranks to avoid the assumption of normality implicit in the analysis of variance. *Journal of the American Statistical Association* 32(200):675–701
24. Fujino A, Ueda N, Saito K (2008) Semisupervised learning for a hybrid generative/discriminative classifier based on the maximum entropy principle. *IEEE Transactions on Pattern Analysis and Machine Intelligence* 30(3):424–437
25. Gacto MJ, Alcalá R, Herrera F (2011) Interpretability of linguistic fuzzy rule-based systems: An overview of interpretability measures. *Information Sciences* 181(20):4340–4360
26. Gilpin LH, Bau D, Yuan BZ, Bajwa A, Specter M, Kagal L (2018) Explaining explanations: An overview of interpretability of machine learning. In: *Proceedings of the IEEE 5th International Conference on Data Science and Advanced Analytics*, IEEE, pp 80–89
27. Gong C, Tao D, Maybank SJ, Liu W, Kang G, Yang J (2016) Multimodal curriculum learning for semi-supervised image classification. *IEEE Transactions on Image Processing* 25(7):3249–3260
28. Gong C, Tao D, Liu W, Liu L, Yang J (2017) Label propagation via teaching-to-learn and learning-to-teach. *IEEE Transactions on Neural Networks and Learning Systems* 28(6):1452–1465
29. Goodfellow I, Pouget-Abadie J, Mirza M, Xu B, Warde-Farley D, Ozair S, Courville A, Bengio Y (2014) Generative adversarial nets. In: *Advances in Neural Information Processing Systems 27*, Curran Associates, Inc., pp 2672–2680
30. Goodman B, Flaxman S (2017) European union regulations on algorithmic decision-making and a right to explanation. *AI Magazine* 38(3):50–57
31. Grau I, Sengupta D, Garcia Lorenzo M, Nowe A (2016) Grey-box model: An ensemble approach for addressing semi-supervised classification problems. In: *Belgian-Dutch Conference on Machine Learning BENELEARN 2016*
32. Grau I, Sengupta D, Garcia Lorenzo M, Nowe A (2018) Interpretable self-labeling semi-supervised classifier. In: Aha D, Darrell T, Doherty P, Daniel Magazzeni (eds) *Proceedings of the 2nd Workshop on Explainable Artificial Intelligence*, International Joint Conference on Artificial Intelligence IJCAI/ECAI 2018, pp 52–57
33. Hady MFA, Schwenker F (2008) Co-training by committee: a new semi-supervised learning framework. In: *Proceedings of the 2008 IEEE International Conference on Data Mining Workshops*, IEEE, pp 563–572
34. Halder A, Ghosh S, Ghosh A (2010) Ant based semi-supervised classification. In: Dorigo M, Birattari M, Di Caro GA, Doursat R, Engelbrecht AP, Floreano D, Gambardella LM, Groß R, Şahin E, Sayama H, Stützle T (eds) *Proceedings of the 7th International Conference on Swarm Intelligence*, Springer, vol LNCS 6234, pp 376–383
35. Hecht-Nielsen R (1989) Theory of the backpropagation neural network. In: *Proceedings of the International Joint Conference on Neural Networks*, IEEE, pp 593–605

36. Holm S (1979) A simple sequentially rejective multiple test procedure. *Scandinavian Journal of Statistics* pp 65–70
37. Japkowicz N, Shah M (2011) *Evaluating learning algorithms: a classification perspective*. Cambridge University Press
38. Karlos S, Fazakis N, Panagopoulou AP, Kotsiantis S, Sgarbas K (2017) Locally application of naive bayes for self-training. *Evolving Systems* 8(1):3–18
39. Keerthi SS, Shevade SK, Bhattacharyya C, Murthy KRK (2001) Improvements to Platt’s SMO algorithm for SVM classifier design. *Neural Computation* 13(3):637–649
40. Kingma DP, Mohamed S, Rezende DJ, Welling M (2014) Semi-supervised learning with deep generative models. In: *Advances in Neural Information Processing Systems 27*, Curran Associates, Inc., pp 3581–3589
41. Lazar C, Meganck S, Taminau J, Steenhoff D, Coletta A, Molter C, Weiss-Solís DY, Duque R, Bersini H, Nowé A (2012) Batch effect removal methods for microarray gene expression data integration: a survey. *Briefings in Bioinformatics* 14(4):469–490
42. Li M, Zhou ZH (2005) Setred: Self-training with editing. In: *Proceedings of the 9th Pacific-Asia Conference on Knowledge Discovery and Data Mining*, Springer, vol LNCS 3518, pp 611–621
43. Li M, Zhou ZH (2007) Improve computer-aided diagnosis with machine learning techniques using undiagnosed samples. *IEEE Transactions on Systems, Man, and Cybernetics Part A: Systems and Humans* 37(6):1088–1098
44. Li Y, Wang Y, Bi C, Jiang X (2018) Revisiting transductive support vector machines with margin distribution embedding. *Knowledge-Based Systems* 152:200 – 214
45. Lipton ZC (2016) The mythos of model interpretability. In: *Proceedings of the 33rd International Conference on Machine Learning. Workshop on Human Interpretability in Machine Learning*, pp 96–100
46. Molnar C (2019) *Interpretable Machine Learning. A Guide for Making Black Box Models Explainable*. Christoph Molnar
47. Nelles O (2013) *Nonlinear system identification: from classical approaches to neural networks and fuzzy models*. Springer
48. Niculescu-Mizil A, Caruana R (2005) Predicting good probabilities with supervised learning. In: *Proceedings of the 22nd International Conference on Machine Learning*, ACM, New York, NY, USA, pp 625–632
49. Odena A (2016) Semi-supervised learning with generative adversarial networks. arXiv preprint arXiv:160601583
50. Oliver A, Odena A, Raffel CA, Cubuk ED, Goodfellow I (2018) Realistic evaluation of deep semi-supervised learning algorithms. In: Bengio S, Wallach H, Larochelle H, Grauman K, Cesa-Bianchi N, Garnett R (eds) *Advances in Neural Information Processing Systems 31*, Curran Associates, Inc., pp 3235–3246
51. Pawlak Z (1982) Rough sets. *International Journal of Computer & Information Sciences* 11(5):341–356

52. Pintelas E, Livieris IE, Pintelas P (2020) A grey-box ensemble model exploiting black-box accuracy and white-box intrinsic interpretability. *Algorithms* 13(1):17
53. Platt J (1999) Probabilistic outputs for support vector machines and comparisons to regularized likelihood methods. *Advances in Large Margin Classifiers* 10(3):61–74
54. Quinlan JR (1993) *C4.5: Programs for machine learning*. Morgan Kaufmann Publishers Inc., San Francisco, CA, USA
55. Salimans T, Goodfellow I, Zaremba W, Cheung V, Radford A, Chen X (2016) Improved techniques for training gans. In: *Advances in Neural Information Processing Systems* 28, Curran Associates, Inc., pp 2234–2242
56. Touw WG, Bayjanov JR, Overmars L, Backus L, Boekhorst J, Wels M, van Hijum SA (2012) Data mining in the life sciences with random forest: a walk in the park or lost in the jungle? *Briefings in Bioinformatics* 14(3):315–326
57. Triguero I, García S, Herrera F (2015) Self-labeled techniques for semi-supervised learning: taxonomy, software and empirical study. *Knowledge and Information Systems* 42(2):245–284
58. Vluymans S, Mac Parthaláin N, Cornelis C, Saeys Y (2016) Fuzzy rough sets for self-labelling: An exploratory analysis. In: *Proceedings of the 2016 IEEE International Conference on Fuzzy Systems, IEEE*, pp 931–938
59. Wainberg M, Alipanahi B, Frey BJ (2016) Are random forests truly the best classifiers? *The Journal of Machine Learning Research* 17(1):3837–3841
60. Weston J, Ratle F, Mobahi H, Collobert R (2012) Deep learning via semi-supervised embedding. In: *Neural Networks: Tricks of the Trade*, vol LNCS 7700, Springer, pp 639–655
61. Wilcoxon F (1945) Individual comparisons by ranking methods. *Biometrics* 1:8083
62. Wilson DR, Martinez TR (1997) Improved heterogeneous distance functions. *Journal of Artificial Intelligence Research* 6:1–34
63. Witten IH, Frank E, Hall MA, Pal CJ (2017) Chapter 11 - Beyond supervised and unsupervised learning, 4th edn, Morgan Kaufmann, pp 467–478
64. Wu D, Luo X, Wang G, Shang M, Yuan Y, Yan H (2018) A highly accurate framework for self-labeled semisupervised classification in industrial applications. *IEEE Transactions on Industrial Informatics* 14(3):909–920
65. Xie Y, Zhang J, Xia Y (2019) Semi-supervised adversarial model for benignmalignant lung nodule classification on chest CT. *Medical Image Analysis* 57:237 – 248
66. Xu W, Tan Y (2019) Semi-supervised target-oriented sentiment classification. *Neurocomputing* 337:120 – 128
67. Yarowsky D (1995) Unsupervised word sense disambiguation rivaling supervised methods. In: *Proceedings of the 33rd Annual Meeting on Association for Computational Linguistics*, Association for Computational Linguistics, Stroudsburg, PA, USA, pp 189–196

68. Yin L, Wang H, Fan W, Kou L, Lin T, Xiao Y (2019) Incorporate active learning to semi-supervised industrial fault classification. *Journal of Process Control* 78:88 – 97
69. Zadrozny B, Elkan C (2001) Obtaining calibrated probability estimates from decision trees and naive bayesian classifiers. In: *Proceedings of the Eighteenth International Conference on Machine Learning*, vol 1, pp 609–616
70. Zhang C, Liu C, Zhang X, Alpanidis G (2017) An up-to-date comparison of state-of-the-art classification algorithms. *Expert Systems with Applications* 82:128–150
71. Zhou Y, Goldman S (2004) Democratic co-learning. In: *Proceedings of the 16th IEEE International Conference on Tools with Artificial Intelligence*, IEEE, pp 594–602
72. Zhou ZH, Li M (2005) Tri-training: Exploiting unlabeled data using three classifiers. *IEEE Transactions on Knowledge and Data Engineering* 17(11):1529–1541
73. Zhu X (2005) Semi-supervised learning literature survey. Tech. Rep. 1530, Computer Sciences, University of Wisconsin-Madison

7 Appendix: Detailed results of statistical tests.

Table 6: Friedman p -values for all ratios when testing different black-box base classifiers. The prediction rates are measured using kappa coefficient. There are significant differences among all the configurations compared.

Ratio	Friedman p -value	H_0
10%	2.10E-08	Rejected
20%	8.91E-13	Rejected
30%	9.87E-06	Rejected
40%	5.35E-04	Rejected

Table 7: Wilcoxon p -values and Holm’s post-hoc correction when comparing different black-boxes configurations. The test supports the superiority of RF as black-box base classifier when comparing prediction rates.

Labeled ratio	Pair of configurations	Wilcoxon p -value	R^-	R^+	Holm	H_0
10%	RF-PART - MLP-PART	2.08E-05	13	39	1.25E-04	Rejected
	RF-PART - SVM-PART	2.77E-04	16	39	1.38E-03	Rejected
	RF-C45 - SVM-C45	6.91E-04	16	39	2.76E-03	Rejected
	RF-RIP - MLP-RIP	9.63E-04	15	40	2.89E-03	Rejected
	RF-C45 - MLP-C45	1.6E-03	15	39	3.2E-03	Rejected
	RF-RIP - SVM-RIP	5.84E-03	19	36	5.84E-03	Rejected
20%	RF-C45 - MLP-C45	5.58E-06	9	45	3.35E-05	Rejected
	RF-PART - SVM-PART	2.1E-05	15	39	1.05E-04	Rejected
	RF-PART - MLP-PART	4.56E-05	13	41	1.83E-04	Rejected
	RF-RIP - SVM-RIP	1.83E-04	17	37	5.5E-04	Rejected
	RF-C45 - SVM-C45	3.04E-04	15	39	6.08E-04	Rejected
	RF-RIP - MLP-RIP	3.56E-03	18	36	3.56E-03	Rejected
30%	RF-RIP - MLP-RIP	1.18E-03	15	38	7.06E-03	Rejected
	RF-C45 - MLP-C45	1.19E-03	16	38	7.06E-03	Rejected
	RF-C45 - SVM-C45	1.75E-03	16	38	7.06E-03	Rejected
	RF-RIP - SVM-RIP	2.93E-03	18	36	8.79E-03	Rejected
	RF-PART - MLP-PART	5.64E-03	20	34	1.13E-02	Rejected
	RF-PART - SVM-PART	7.7E-03	20	34	1.13E-02	Rejected
40%	RF-RIP - SVM-RIP	1.55E-03	16	38	9.33E-03	Rejected
	RF-PART - MLP-PART	6.26E-03	19	35	3.13E-02	Rejected
	RF-C45 - MLP-C45	8.75E-03	20	34	3.5E-02	Rejected
	RF-PART - SVM-PART	1.43E-02	19	35	4.29E-02	Rejected
	RF-C45 - SVM-C45	2.28E-02	22	32	4.55E-02	Rejected
	RF-RIP - MLP-RIP	7.68E-02	23	31	7.68E-02	Not Rejected

Table 8: Friedman p -values for all ratios when testing the prediction performance (kappa) for different white-box and amending configurations. There are statistical differences in the prediction rates in at least one pair of the configurations compared.

Ratio	Friedman p -value	H_0
10%	4.02E-07	Rejected
20%	9.27E-07	Rejected
30%	1.67E-03	Rejected
40%	7.35E-05	Rejected

Table 9: Wilcoxon p -values and Holm's post-hoc correction when comparing different white-box and amending configurations. Per ratio, first subsection compares using different amending procedures while fixing the white box and the second subsection fixes the amending for comparing the influence of white boxes. The vast majority of null hypothesis cannot be rejected, indicating that amending or white-box alternatives do not strongly influence the prediction rates.

Labeled ratio	Pair of configurations	Wilcoxon p -value	R^-	R^+	Holm	H_0	
10%	RF-RIP-RST - RF-RIP-NONE	2.57E-03	40	12	1.54E-02	Rejected	
	RF-C45-RST - RF-C45-NONE	3.4E-02	36	17	0.170	Not Rejected	
	RF-RIP-CONF - RF-RIP-NONE	4.23E-02	33	19	0.170	Not Rejected	
	RF-PART-RST - RF-PART-NONE	5.24E-02	31	21	0.170	Not Rejected	
	RF-C45-CONF - RF-C45-NONE	0.224	30	23	0.447	Not Rejected	
	RF-PART-CONF - RF-PART-NONE	0.344	27	25	0.447	Not Rejected	
	RF-RIP-CONF - RF-PART-CONF	7.09E-04	35	18	6.38E-03	Rejected	
	RF-RIP-RST - RF-PART-RST	1.44E-02	35	18	0.115	Not Rejected	
	RF-RIP-NONE - RF-PART-NONE	1.97E-02	34	19	0.138	Not Rejected	
	RF-RIP-RST - RF-C45-RST	2.01E-02	33	20	0.138	Not Rejected	
	RF-RIP-CONF - RF-C45-CONF	3.25E-02	33	20	0.163	Not Rejected	
	RF-PART-CONF - RF-C45-CONF	9.52E-02	18	33	0.381	Not Rejected	
	RF-PART-NONE - RF-C45-NONE	0.166	23	29	0.499	Not Rejected	
	RF-PART-RST - RF-C45-RST	0.188	20	30	0.499	Not Rejected	
	RF-RIP-NONE - RF-C45-NONE	0.510	31	23	0.510	Not Rejected	
	20%	RF-RIP-RST - RF-RIP-NONE	8.04E-05	38	14	4.82E-04	Rejected
		RF-C45-CONF - RF-C45-NONE	4.89E-03	36	14	2.45E-02	Rejected
		RF-PART-RST - RF-PART-NONE	4.92E-02	33	19	0.197	Not Rejected
RF-PART-CONF - RF-PART-NONE		5.23E-02	33	18	0.197	Not Rejected	
RF-C45-RST - RF-C45-NONE		5.82E-02	34	18	0.197	Not Rejected	
RF-RIP-CONF - RF-RIP-NONE		0.169	31	21	0.197	Not Rejected	
RF-RIP-RST - RF-PART-RST		1.6E-03	39	14	1.44E-02	Rejected	
RF-RIP-RST - RF-C45-RST		6.12E-03	36	16	4.9E-02	Rejected	
RF-RIP-NONE - RF-PART-NONE		2.78E-02	36	17	0.195	Not Rejected	
RF-RIP-NONE - RF-C45-NONE		4.53E-02	36	18	0.272	Not Rejected	
RF-RIP-CONF - RF-C45-CONF		0.169	30	22	0.854	Not Rejected	
RF-RIP-CONF - RF-PART-CONF		0.259	28	25	1.000	Not Rejected	
RF-PART-RST - RF-C45-RST		0.769	26	23	1.000	Not Rejected	
RF-PART-NONE - RF-C45-NONE		0.827	27	25	1.000	Not Rejected	
RF-PART-CONF - RF-C45-CONF		0.889	27	23	1.000	Not Rejected	
30%		RF-RIP-RST - RF-RIP-NONE	2.18E-04	37	15	1.31E-03	Rejected
		RF-C45-RST - RF-C45-NONE	8.45E-03	37	16	4.22E-02	Rejected
		RF-RIP-CONF - RF-RIP-NONE	4.14E-02	32	20	0.165	Not Rejected
	RF-C45-CONF - RF-C45-NONE	0.193	28	24	0.578	Not Rejected	
	RF-PART-CONF - RF-PART-NONE	0.362	28	24	0.725	Not Rejected	
	RF-PART-RST - RF-PART-NONE	0.388	28	25	0.725	Not Rejected	
	RF-RIP-RST - RF-PART-RST	1.68E-03	37	15	1.51E-02	Rejected	
	RF-RIP-RST - RF-C45-RST	7.03E-03	35	17	5.62E-02	Not Rejected	
	RF-RIP-CONF - RF-C45-CONF	0.147	30	24	1.000	Not Rejected	
	RF-PART-RST - RF-C45-RST	0.259	22	27	1.000	Not Rejected	
	RF-RIP-CONF - RF-PART-CONF	0.324	30	24	1.000	Not Rejected	
	RF-RIP-NONE - RF-PART-NONE	0.355	31	22	1.000	Not Rejected	
	RF-RIP-NONE - RF-C45-NONE	0.498	28	25	1.000	Not Rejected	
	RF-PART-NONE - RF-C45-NONE	0.555	22	29	1.000	Not Rejected	
	RF-PART-CONF - RF-C45-CONF	0.573	23	25	1.000	Not Rejected	
	40%	RF-RIP-RST - RF-RIP-NONE	1.35E-05	40	13	8.13E-05	Rejected
		RF-RIP-CONF - RF-RIP-NONE	7.03E-03	31	21	3.51E-02	Rejected
		RF-PART-RST - RF-PART-NONE	0.136	30	23	0.543	Not Rejected
RF-PART-CONF - RF-PART-NONE		0.579	28	24	1.000	Not Rejected	
RF-C45-RST - RF-C45-NONE		0.662	26	26	1.000	Not Rejected	
RF-C45-CONF - RF-C45-NONE		0.761	26	24	1.000	Not Rejected	
RF-RIP-RST - RF-C45-RST		2.9E-03	39	13	2.61E-02	Rejected	
RF-RIP-CONF - RF-PART-CONF		2.13E-02	36	18	0.170	Not Rejected	
RF-RIP-CONF - RF-C45-CONF		3.25E-02	33	20	0.228	Not Rejected	
RF-RIP-RST - RF-PART-RST		3.96E-02	33	20	0.237	Not Rejected	
RF-RIP-NONE - RF-PART-NONE		0.254	33	21	1.000	Not Rejected	
RF-PART-NONE - RF-C45-NONE		0.267	23	30	1.000	Not Rejected	
RF-PART-CONF - RF-C45-CONF		0.606	26	24	1.000	Not Rejected	
RF-RIP-NONE - RF-C45-NONE		0.806	29	23	1.000	Not Rejected	
RF-PART-RST - RF-C45-RST		0.858	26	24	1.000	Not Rejected	

Table 10: Friedman p -values for all ratios when comparing the interpretability in terms of simplicity, for different white-box and amending configurations. There are significant differences among all the configurations compared, where RF-RIP-RST exhibits the highest mean for all ratios (see Table 4).

Ratio	Friedman p -value	H_0
10%	3.14E-73	Rejected
20%	3.02E-75	Rejected
30%	3.96E-72	Rejected
40%	2.41E-71	Rejected

Table 11: Wilcoxon p -values and Holm's post-hoc correction when comparing different white-box and amending configurations against the highest mean simplicity combination: RF-RIP-RST. All null hypothesis can be safely rejected, showing statistically significant superiority in terms of simplicity.

Labeled ratio	Pair of configurations	Wilcoxon p -value	R^-	R^+	Holm	H_0
10%	RF-RIP-RST - RF-C45-NONE	1.11E-10	0	55	8.86E-10	Rejected
	RF-RIP-RST - RF-PART-NONE	1.17E-10	1	54	8.86E-10	Rejected
	RF-RIP-RST - RF-C45-CONF	1.63E-10	0	54	9.75E-10	Rejected
	RF-RIP-RST - RF-C45-RST	1.63E-10	0	54	9.75E-10	Rejected
	RF-RIP-RST - RF-RIP-NONE	2.39E-10	0	53	9.75E-10	Rejected
	RF-RIP-RST - RF-PART-CONF	3.97E-10	2	52	1.19E-09	Rejected
	RF-RIP-RST - RF-PART-RST	4.08E-09	3	51	8.17E-09	Rejected
	RF-RIP-RST - RF-RIP-CONF	2.18E-07	5	46	2.18E-07	Rejected
20%	RF-RIP-RST - RF-C45-NONE	1.11E-10	0	55	8.86E-10	Rejected
	RF-RIP-RST - RF-PART-NONE	1.11E-10	0	55	8.86E-10	Rejected
	RF-RIP-RST - RF-C45-CONF	1.11E-10	0	55	8.86E-10	Rejected
	RF-RIP-RST - RF-PART-CONF	1.11E-10	0	55	8.86E-10	Rejected
	RF-RIP-RST - RF-C45-RST	1.63E-10	0	54	8.86E-10	Rejected
	RF-RIP-RST - RF-RIP-NONE	2.39E-10	0	53	8.86E-10	Rejected
	RF-RIP-RST - RF-RIP-CONF	8.76E-10	1	52	1.75E-09	Rejected
	RF-RIP-RST - RF-PART-RST	3.95E-08	3	50	3.95E-08	Rejected
30%	RF-RIP-RST - RF-C45-NONE	1.11E-10	0	55	8.86E-10	Rejected
	RF-RIP-RST - RF-C45-CONF	1.11E-10	0	55	8.86E-10	Rejected
	RF-RIP-RST - RF-PART-NONE	1.24E-10	1	54	8.86E-10	Rejected
	RF-RIP-RST - RF-C45-RST	1.24E-10	1	54	8.86E-10	Rejected
	RF-RIP-RST - RF-PART-CONF	1.31E-10	2	53	8.86E-10	Rejected
	RF-RIP-RST - RF-RIP-NONE	2.6E-10	1	52	8.86E-10	Rejected
	RF-RIP-RST - RF-RIP-CONF	8.03E-10	1	49	1.61E-09	Rejected
	RF-RIP-RST - RF-PART-RST	1.18E-09	3	51	1.61E-09	Rejected
40%	RF-RIP-RST - RF-C45-NONE	1.11E-10	0	55	8.86E-10	Rejected
	RF-RIP-RST - RF-C45-CONF	1.11E-10	0	55	8.86E-10	Rejected
	RF-RIP-RST - RF-PART-NONE	1.24E-10	1	54	8.86E-10	Rejected
	RF-RIP-RST - RF-PART-CONF	1.31E-10	1	54	8.86E-10	Rejected
	RF-RIP-RST - RF-C45-RST	1.63E-10	0	54	8.86E-10	Rejected
	RF-RIP-RST - RF-RIP-NONE	2.68E-10	1	52	8.86E-10	Rejected
	RF-RIP-RST - RF-RIP-CONF	3.18E-10	2	51	8.86E-10	Rejected
	RF-RIP-RST - RF-PART-RST	2.7E-09	4	51	2.7E-09	Rejected

Table 12: Friedman p -values for all ratios when comparing SIGb (RF-PART-RST) with state-of-the-art semi-supervised classifiers in terms of prediction rates (kappa). There are significant differences for all ratios, where SIGb exhibits the highest mean (see Table 5).

Ratio	Friedman p -value	H_0
10%	1.91E-06	Rejected
20%	7.62E-07	Rejected
30%	3.50E-06	Rejected
40%	2.19E-03	Rejected

Table 13: Wilcoxon p -values and Holm's post-hoc correction using SIGb approach as control method against state-of-the-art semi-supervised classifiers. SIGb significantly outperforms other methods except for CT(SMO) and DCT when using 30% and 40% of labeled instances.

Labeled ratio	SSC algorithm	Wilcoxon p -value	R^-	R^+	Holm	H_0
10%	CB(C45)	3.6E-06	12	43	1.44E-05	Rejected
	TT(C45)	4.23E-06	13	42	1.44E-05	Rejected
	DCT	1.86E-05	12	43	3.71E-05	Rejected
	CT(SMO)	1.74E-04	16	39	1.74E-04	Rejected
20%	CB(C45)	1.3E-07	9	46	5.21E-07	Rejected
	TT(C45)	8.37E-07	9	46	2.51E-06	Rejected
	DCT	2.77E-04	15	40	5.53E-04	Rejected
	CT(SMO)	2.35E-03	19	36	2.35E-03	Rejected
30%	CB(C45)	1.64E-07	9	46	6.54E-07	Rejected
	TT(C45)	4.84E-07	9	45	1.45E-06	Rejected
	DCT	7.16E-03	19	36	1.43E-02	Rejected
	CT(SMO)	5.4E-02	20	35	5.4E-02	Not Rejected
40%	TT(C45)	6.58E-05	12	42	2.63E-04	Rejected
	CB(C45)	8.18E-05	15	39	2.63E-04	Rejected
	DCT	0.172	24	31	0.344	Not Rejected
	CT(SMO)	0.633	27	28	0.633	Not Rejected